Jurnal
Teknologi

Full Paper

TURBULENT-FORCED CONVECTIVE HEAT TRANSFER AND PRESSURE DROP ANALYSIS OF FE3O4 MAGNETIC NANOFLUID IN A CIRCULAR MICROCHANNEL

Nor Azwadi Che Sidik*, M.M. Yassin, M.N.Musa

Faculty of Mechanical Engineering, Universiti Teknologi Malaysia, 81310 UTM Johor Bahru, Johor, Malaysia

Article history
Received
18 Feb 2015
Received in revised form
19 March 2015
Accepted
25 March 2015

*Corresponding author
azwadi@fkm.utm.my

Graphical abstract

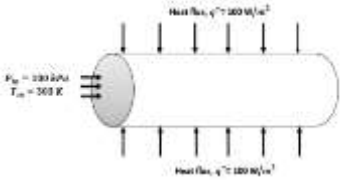

Abstract

A numerical simulation was accomplished in this study that investigated the turbulent force convective heat transfer and pressure drop in straight circular copper pipe with a hydraulic diameter of 0.0005m and 0.1m in length, as given by Lee and Mudawar [11]. The enhancement of heat transfer for water and nanofluids (Fe3O4) under 100 [W/m2] constant heat flux was applied around the wall of the pipe. In this study, standard k-ε turbulence model was employed and was performed at a steady state flow, incompressible turbulent flow, and three-dimensional structure. Various volume concentrations of nanoparticles were conducted in the range of 1% to 15% at constant nanoparticle diameter size, which was 32 nm. The heat transfer enhancement was obtained in the range of Reynolds number from 3000 to 10,000. The results displayed an increase in Reynolds number and volume concentrations, as well as an increase in the Nusselt number. The optimum Nusselt number gained was about 5% to 6% of volume concentration at each Reynolds number tested. Besides, with the increase of Reynolds number, the variation pressure saw a dropped for inlet, whereas an increase in the outlet section. Moreover, the increase in volume concentration also caused a small increment in the pressure drop compared to pure water.

Keywords: Microchannel; turbulent flow; nanofluid; forced convection

Abstrak

Simulasi berangka telah dicapai dalam kajian ini yang menyiasat daya perolakan pemindahan gelora haba dan kejatuhan tekanan dalam paip lurus tembaga bulat dengan diameter hidraulik 0.0005m dan 0.1m panjang yang diberikan oleh Lee dan Mudawar [11]. Peningkatan dalam pemindahan haba untuk air dan nanofluids (Fe3O4) adalah di bawah 100 [W / m2] fluks haba tetap digunakan di seluruh dinding paip. Dalam kajian ini, standard k-ε model gelora telah digunakan dan dilakukan pada aliran mantap, aliran gelora tak boleh mampat, dan struktur tiga dimensi. Pelbagai kepekatan nanopartikel dikaiji antara 1% hingga 15% di nanopartikel dengan saiz diameter 32 nm. Peningkatan pemindahan haba telah diperolehi dalam pelbagai nombor Reynolds dari 3000 kepada 10,000. Hasil kajian menunjukkan peningkatan bilangan dan jumlah kepekatan Reynolds, serta nombor Nusselt. Bilangan Nusselt optimum adalah kira-kira 5% kepada jumlah kepekatan 6% pada setiap nombor Reynolds yang diuji. Selain peningkatan bilangan Reynolds, kajian menunjukkan penurunan tekanan variasi untuk bahagian masuk dan penurunan di bahagian keluar. Peningkatan dalam kepekatan juga menyebabkan kenaikan kecil dalam kejatuhan tekanan jika dibandingkan dengan air tulen.

Kata kunci: Mikro ; Aliran bergelora ; nanofluid ; olakan dipaksa

1.0 INTRODUCTION

Over the last two decades, the importance of micromachining technology had increased dramatically as it has been used for the development of highly efficient cooling devices. Microchannel is one of the essential parts to dissipate high heat fluxes in microelectromechanical-system. Thus, an extensive study on fluid flow and heat transfer in the microchannel heat transfer was proposed by pioneering work of Tuckerman and Pease [1] in 1981. Besides, turbulent convection in microchannels is believed as an effective cooling mechanism for high power density systems [2, 3]. Besides, Wu and Cheng [4], and Qu and Mudawar [5] stated that microchannel provides a very high surface area to volume ratio, small coolant requirement, large heat transfer coefficient, as well as very small mass and volume per heat load.

A new generation of fluids with nanoparticles suspended in them is called nanofluids, which was introduced by Choi in 1995 [6]. The modern heat carrier consisted of nanosize solid particles, such as copper, aluminium, and their oxides, whereby less than 100 nm was dispersed into base fluids to change their thermal conductivity and viscosity. Moreover, many researchers have investigated experimentally [7] and numerically [8] confirmed that the nanofluids can bring heat transfer enhancement. One of the ways observed has been by increasing the volume of concentration.

In addition, Chein and Chuang [9] also conducted a study of microchannel heat sink performance using CuO-H2O in the range of volume fraction between 0.2 and 0.4%. The experimental result indicated that the nanofluids could absorb more heat and attained lower wall temperatures than pure liquid. There was also a slight effect in the increase in pressure drop compared to pure liquid cooled.

Other than that, Yeul Jung [10] used Al2O3 particles at a diameter of 170 nm with several volume fractions of 0.6%, 1.2%, and 1.8%. About 32% of increase of heat transfer coefficient of Al2O3 was compared to distilled water at 1.8% of volume fraction in laminar regime. They also discovered an increment in the Nusselt numbers with the increase in Reynold numbers.

Meanwhile, Lee and Mudawar [11] experimentally conducted the effectiveness of Al2O3-water for single-phase and two-phase heat transfer. As for single-phase, heat transfer coefficient was increased because the high thermal conductivity of nanofluids. The enhancement was quite weak in the fully developed region because of the effect of thermal boundary layer development. Besides, they found that the two-phase cannot be applied to microchannel because of catastrophic failure.

2.0 MATHEMATICAL MODELLING

2.1 Governing Equations

In this work, 3D computational fluid dynamic (CFD) was developed. The Governing equation, i.e. continuity, momentum, and energy, are presented in the following [12];

Continuity equation:

$$\frac{\delta}{\delta x_j}(\rho u_j) = 0 \tag{1}$$

Momentum equation:

$$\frac{\delta}{\delta x_j}(\rho u_i u_j) = \frac{\delta p}{\delta x_j} + \frac{\delta}{\delta x_j}\left[(\mu + \mu_t)\frac{\delta}{\delta x_j}\right] + \frac{\delta}{\delta x_j}\left[(\mu + \mu_t)\frac{\delta}{\delta x_j}\right] \tag{2}$$

Energy equation:

$$\frac{\delta}{\delta x_j}(\rho u_j T) = \frac{\delta}{\delta x_j}\left[\left(\frac{1}{C_p} + \frac{\mu_t}{\sigma_t}\right)\frac{\delta T}{\delta x_j}\right] \tag{3}$$

On top of that, standard k-ε turbulent model was applied, as the equation of turbulent kinetic energy (k) and the rate of dissipation (ε) were defined [12];

$$\frac{\delta}{\delta t}(\rho k) + \frac{\delta}{\delta x_j}(\rho k u_j) = \frac{\delta}{\delta x_j}\left[\left(\mu + \frac{\mu_t}{\sigma_k}\right)\frac{\delta k}{\delta x_j}\right] + G_k + \rho\varepsilon \tag{4}$$

$$\frac{\delta}{\delta t}(\rho\varepsilon) + \frac{\delta}{\delta x_j}(\rho\varepsilon u_j) = \frac{\delta}{\delta x_j}\left[\left(\mu + \frac{\mu_t}{\sigma_\varepsilon}\right)\frac{\delta\varepsilon}{\delta x_j}\right] + C_{1\varepsilon}\frac{\varepsilon}{k}(G_k) - C_{2\varepsilon}\rho\frac{\varepsilon^2}{k} \tag{5}$$

μ, is the eddy viscosity and it is defined as;

$$\mu_t = \rho C_\mu \frac{k^2}{\varepsilon} \tag{6}$$

Where Gk represents the generation of turbulent kinetic energy due to mean velocity gradients, σk=1.0 and $\sigma\varepsilon$= 1.3 are turbulent Prandtl numbers for the kinetic energy, and its dissipation rates, $C1\varepsilon$=1.44, $C2\varepsilon$=1.92, and $C\mu$= 0.09 are default values. All values that were constant had been proven experimentally.

2.2 Thermophysical of Nanofluids

The effective thermophysical of magnetic nanofluids Fe3O4 are given in the following [13];

Effective density of nanofluids:

$$\rho_{nf} = (1-\phi)\rho_{bf} + \phi\rho_p \quad (7)$$

Effective capacity nanofluids:

$$C_{nf} = \frac{\phi\rho_p C_p + (1-\phi)\rho_{bf} C_{bf}}{\rho_{nf}} \quad (8)$$

Effective thermal conductivity nanofluids:

$$k_{nf} = k_{bf}\left(\frac{k_p + 2k_{bf} - 2\phi(k_{bf} - k_p)}{k_p + 2k_{bf} + \phi(k_{bf} - k_p)}\right) \quad (9)$$

Effective dynamic viscosity nanofluids:

$$\mu_{nf} = \frac{\mu_{bf}}{(1-\phi)^{2.5}} \quad (10)$$

Where nf is nanofluids, bf is base fluids (water), and p is nanoparticle (Fe3O4)

2.3 Assumptions and Boundary Conditions

Fig. 1 shows a 3D circular channel with 0.0005m diameter and 1m length, which had been investigated. The wall was applied with constant heat flux at 100 [W/m2]. The geometry was enclosed by an inlet surface, outlet surface with inlet temperature, Tin = 303 K, and inlet pressure at Pin = 100 kPa. Besides, the inlet velocity applied had been uin=ui, uj= 0,, and there was no slip in hydraulic boundary condition of velocity at wall.

The nanofluids that consisted of Fe3O4 particles at 36 nm average diameter size was used. Different volume concentrations (1-15%) were tested at a range of Reynolds number from 3000 to 10,000. The simulation study was assumed as in the following:

i. The flow was forced convection turbulence flow.
ii. Single-phase.
iii. Steady state.
iv. Incompressible flow.
v. Fully developed flow.

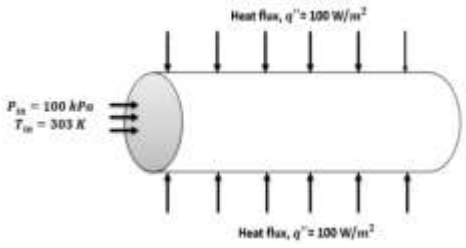

Figure 1 Geometry of circular pipe applied to workbench.

3.0 RESULTS AND DISCUSSION

The results were analyzed using water and nanofluids (at volume concentrations of 1%, 3%, 6%, 10%, and 15%). The heat transfer coefficient, Nusselt number, and pressure drop were calculated with eqns. 11-13 respectively;

$$\hat{h}_{avg} = \frac{q''}{T_w - T_b}\left(W/m^2.K\right) \quad (11)$$

$$Nu_{avg} = \frac{\hat{h}D_h}{k} \quad (12)$$

$$\Delta P = P_{avg,in} - P_{avg,out} \ [Pa] \quad (13)$$

where is heat flux, Tw and Tb are wall temperature and bulk temperature respectively. is heat transfer coefficient, Dh is hydraulic diameter, and k is thermal conductivity. Meanwhile, $Pavg$, and $Pavg$, are total pressure at inlet and outlet respectively.

3.1 Validation of Forced Convection

Validation and precision of the model, as well as numerical procedure, were demonstrated by the comparison of the numerical friction factor with the Darcy friction correlation given by Blasius [14] formula as given in Eq. (14). As shown in Fig. 2, the friction factor decreased with the increase in Reynolds numbers in pure water.

$$f = 4C_f = 4\left(0.079\,\mathrm{Re}^{-\frac{1}{4}}\right) \quad (14)$$

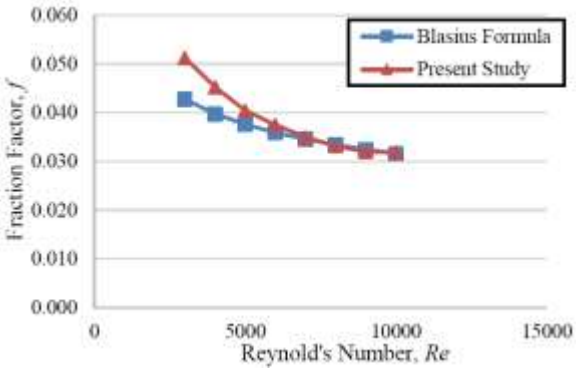

Figure 2 Comparison of darcy fraction factor with numerical value of water at various reynolds number.

Next, the calculated Nusselt number of pure water at a range of study for Reynolds numbers was compared to the correlation given by Gnielinski [15] (Eqn. 15) in Fig. 3. Besides, the calculated Nusselt number is given by Eqn. (12). It had been observed that the Nusselt number increased with the increase in Reynolds number. The error obtained for comparison

to Gnielinski correlation of water was a maximum error of 13.1%.

$$Nu = 0.012\left(Re^{0.87} - 280\right)Pr^{0.4} \quad (15)$$

$$3\times10^{3} \le Re \le 10^{6}$$

$$1.5 \le Pr \le 500$$

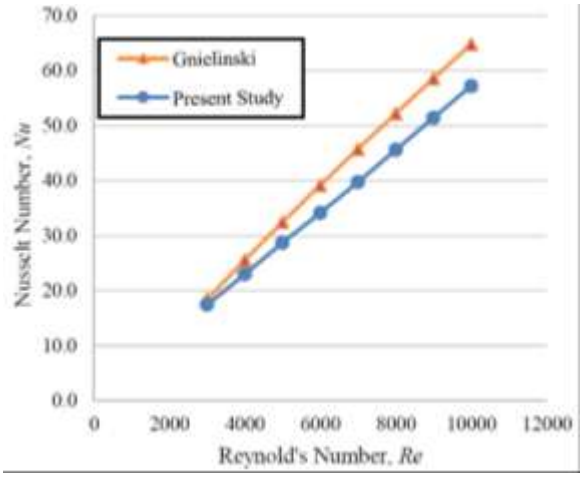

Figure 3 Simulation results of Nusselt number of water in comparison with Gnielinski

3.2 Effects of Nanoparticle Volume / Concentration of Average Nusselt Number

Fig. 4 represents the Nusselt number versus Reynolds number for various volume concentrations of nanoparticles. As observed, in general and despite of some dispersions noticed on the computed value of the Nusselt number, it had been obvious that the increase in Reynolds number and volume concentration of nanofluids increased the value of Nusselt number. Nanofluids with higher particle concentration had higher effective thermal conductivities, which in turn, increased the heat transfer coefficient. Besides, this was also due to the increase in the Prandtl number.

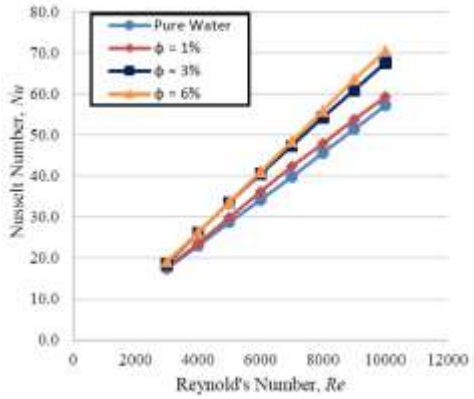

Figure 4 Effects of nanofluids concentration and reynold number on the nusselt number

3.3 Optimum Nusselt Number of Volume Concentration

Fig. 5 explains the case of decrements in Nusselt number. It had been obvious that the Nusselt number optimized at certain values of volume concentration. For example, for Reynolds number 10,000, the volume concentration was around 5% to 6%, which gave an optimum Nusselt number of 69. Besides, the same volume concentration results of Reynolds number of 7000, 8000, and 9000 contributed to an optimum value of the Nusselt number at about 47, 55, and 62, respectively.

Meanwhile, the onset decomposition temperature for regenerated cellulose was 35 °C lower than the cellulose. Thermal stability of regenerated cellulose was reduced after regeneration process. This can be explained as most of the hydrogen bonds and cellulose molecular chains were degraded by NaOH, thus reduced the molecular weight and crystallinity[8]. Low molecular weight accelerates the thermal degradation process. This is consistent with the result obtained by Chen et al. (2011). They found that the regenerated cellulose membrane prepared by ionic liquid had lower thermal stability than the original cellulose. Even though regenerated cellulose had a lower onset decomposition temperature, it gave higher residual mass after the decomposition process. This result indicated that the regenerated cellulose gave higher char yield (non-volatile carbonaceous material) on pyrolysis stage[8].

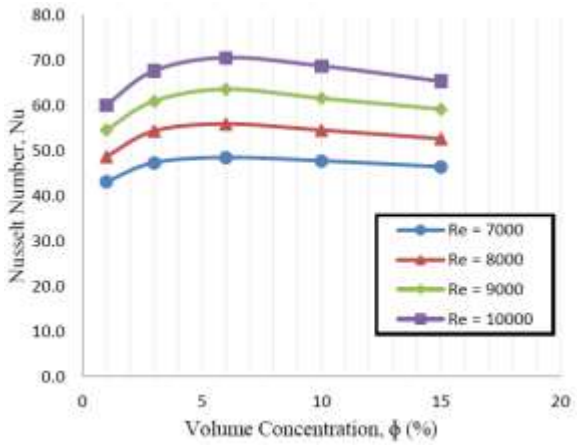

Figure 5 Optimum volume concentration on nusselt number at certain reynolds number.

Fig. 6 shows the variation of the measured pressure drop between the inlet and the outlet circular pipe with Reynolds number. A particle concentration dependency is shown with the total pressure increase with the increase in nanoparticles concentration. The increase in pressure drop was rather high in amount of value than pure water in the microchannel, which causes a small extra penalty in pumping power in engineering application.

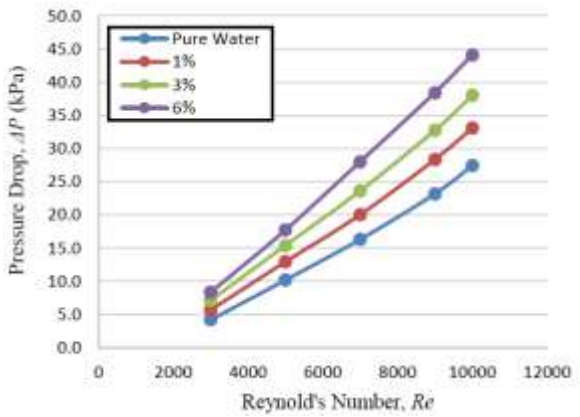

Figure6 Pressure drop comparison between pure water and nanofluids

4.0 CONCLUSION

In this study, a numerical investigation was carried out on the effect of volume concentration on the average Nusselt number and pressure drop. The volume concentration was determined to identify the optimum Nusselt number in the range of Reynolds number tested. The result of the study showed that;

i. The result showed the insufficient agreement or small error of correlation for Nusselt number and fraction factor of pure water, but they were acceptable since the error was less than 15%.
ii. The surface heat transfer coefficient increased as the Reynolds number increased, as well as the increase in volume concentration.
iii. With the increase of Reynolds number and volume concentrations, the Nusselt number increased as well.
iv. The optimum Nusselt number gained was about 5% to 6% of volume concentration at each Reynolds number tested.
v. The rapid enhancement of heat transfer coefficient was in the range of volume concentration of 1% to 3% at Reynolds number tested.
vi. With the increase of Reynolds number, the variation pressure dropped for inlet, while the outlet section increased. Besides, the increase of volume concentration caused a small increment in pressure drop than pure water.
vii. The new correlation of water was obtained at Nu = 0.0146 Re0.8 Pr0.5, which was valid to $3000 \leq Re \leq 10{,}000$ and $Pr \geq 5.45$

Acknowledgement

The authors wish to thank Universiti Teknologi Malaysia.

References

[1] D. B. Tuckerman, R. F. Pease.1981. High-performance heat sinking for VLSL, IEEE Electronic *Devices Letters* 2: 126-129.
[2] K. Azar. 2003, "Cooling Technologies Option, Part 1 and 2", *Electronics*. 9(3): 10-14 (Part 1); *Electronic Cooling*. 9(4): 30-36 (Part 2).
[3] M. J. Ellsworth Jr., S. Simons. 2005, High powered chip cooling-air and beyond. *Electronic Cooling*. 3: 14-22.
[4] H. Y. Wu, P. Cheng. 2003. Experimental study of convective heat transfer in silicon microchannel with different surface condition. *Int. J. Mass Heat Transfer*. 46: 2537-2556.
[5] W. Qu, I. Mudawar. 2002. Experimental and numerical study of pressure drop and heat transfer in a single-phase microchannel heat sink. *Int. J. Heat Transfer*. 45: 259-265.
[6] S. U. S. Choi. 1998. Enhancing thermal conductivity of fluids with nanoparticles, In:*Proceeding of the 1995 ASME Int. Mechanical Engineering Congress and Exposition*, ASME, New York. 99-105.
[7] B. C. Pak,Y. I. Cho. 1998. Hydrodynamic and heat transfer study of dispersed fluid with submicron metallic oxide particle. *Experimental Heat Transfer*. 11: 151-170.
[8] S. E. B. Maiga, S. J.Palm, C. T.Nguyen. 2005. Heat transfer enhancement by using nanofluids in forced convection flow. *Int. Journal of Heat and Fluid Flow* .26: 530-546.
[9] R. Chein, J. Chuang. 2006. experimental microchannel heat sink performance studies using nanofluids. *Int. J. of Thermal Sciences*. 46: 57-66.
[10] J-Y. Jung, Oh. Hoo-Suk et al. 2009. Forced convective heat transfer of nanofluids in microchannels. *Int. J. of Heat and Mass Transfer* 52: 466-472.
[11] J. Lee, I. Mudawar. 2007. Assessment of the effectiveness of nanofluids for single-phase and two-phase heat transfer in micro-channels. Int. *J. of Heat and Mass Transfer*. 50: 452-463.
[12] M. Rostamani, S. F. Hosseinizadeh et al. 2010. Numerical study of turbulent forced convection flow of nanofluids in a long horizontal duct considering variable properties, *Int. Communications in Heat and Mass Transfer*. 37: 1426-1431.
[13] M. K. Moraveji, M. Hekazian. 2012. Modelling of turbulent forced convective heat transfer and friction factor in a tube for Fe3O4 magnetic nanofluids with computational fluids dynamics. *Int. Communications in Heat and Mass Transfer* 39: 1293-1296.
[14] F. P. Incropera, D. P. De Witt. 2002. *Fundamentals of Heat and Mass Transfer*. John Wiley and Sons, New York, USA.
[15] V. Gnielenski. 1976. New equations for heat and mass transfer in turbulent pipe and channels flow. *Int. Chemical Engineering* 16: 359-368.